American Mineralogist, Volume 91, pages 826–830, 2006

Stabilizing of methane hydrate and transition to a new high-pressure structure at 40 GPa

HISAKO HIRAI,[1,*] SHIN-ICHI MACHIDA,[1] TARO KAWAMURA,[2] YOSHITAKA YAMAMOTO,[2] AND TAKEHIKO YAGI[3]

[1]Graduate School of Life and Environmental Science, University of Tsukuba, Tsukuba, Ibaraki, 305-8572, Japan
[2]National Institute of Advanced Industrial Science and Technology, Tsukuba, Ibaraki 305-8569, Japan
[3]Institute for Solid State Physics, Tokyo University, 5-1-5 Kashiwanoha, Kashiwa, Chiba 277-8581, Japan

ABSTRACT

High-pressure experiments of methane hydrate with a composition of full-occupancy of structure I were performed in a pressure range from 0.2 to 86 GPa. X-ray diffractometry and Raman spectroscopy revealed that methane hydrate transformed from a known high-pressure structure, filled-ice-Ih structure, to a new high-pressure structure at approximately 40 GPa. The reason for the outstanding retention of the filled-ice-Ih structure up to 40 GPa was examined, because the filled-ice-Ih structures for other gas hydrates decompose below 6.5 GPa. In the Raman spectra, new intramolecular vibration modes softer than the original ones appeared at 14 to 17 GPa, indicating that additional intermolecular interaction arose around the methane molecules. The additional interaction might be induced by symmetrization of the hydrogen bonds forming the framework. The symmetrization of the framework and the subsequent additional interactions between the methane molecules and the framework water molecules and also between the methane molecules are likely the cause of the excellent stabilization. The new high-pressure structure survived at least to 86 GPa.

Keywords: Methane hydrate, high-pressure study, phase transition, Raman spectroscopy, XRD data, crystal structure

INTRODUCTION

Methane hydrate, called fiery ice, is expected to be a clean and fruitful energy resource, while methane is a greenhouse gas even more potent than carbon dioxide (Sloan 1998; Kvenvolden 1988). During the evolution of the earth, catastrophic climate-changes have been related to the effects of methane hydrate, e.g., an extinction event at the Permian-Triassic boundary (Olszewski and Erwin 2004) and recovery from "snowball earth" in the Neoproterozoic (Hoffman et al. 1998; Jiang et al. 2003). In the solar system, methane hydrate is thought to be an important constituent of outer giant planets and their satellites, such as Uranus, Neptune, and Titan (e.g., Hubbard 1997). Therefore, knowledge of the stability and structural changes of methane hydrate under a wide range of pressure-temperature conditions is required from various standpoints for overcoming humankind's urgent problems of dwindling energy resources and global warming, as well as for answering fundamental questions about the internal structure and evolution of the icy planetary bodies.

Comprehensive studies performed so far under relatively lower pressures have contributed greatly to basic understanding and practical use of methane hydrate (e.g., Sloan 2004; Wait et al. 2004; Circone et al. 2004; Sloan 1998; Stern et al. 1996; Ripmeester et al. 1987; Jeffrey 1984). High-pressure studies of gas hydrates, including methane hydrate, carried out in the last few years have developed our knowledge of the structural changes in gas hydrates under pressures below 10 GPa (e.g., Loveday et al. 2001a; Hirai et al. 2001; Mao et al. 2002). An outline of the structural changes depending on guest size and pressure has been presented for guest sizes up to 4.5 A (Hirai et al. 2004). In the case of methane hydrate, the initial cubic structure I (sI) transforms to a hexagonal structure (sH) at about 1 GPa, and it further transforms to a filled-ice-Ih structure at about 2 GPa (Chou et al. 2000; Hirai et al. 2001; Loveday et al. 2001a; Shimizu et al. 2002). The filled-ice-Ih structure (FIIhS) consists not of cages as for the former two structures, but of channels formed by water molecules and filled with guest species (Loveday et al. 2001b). The other gas hydrates, having guest sizes from that of argon to nitrogen, finally transform to the common FIIhS, although their initial and intermediate structures are different (Kurnosov et al. 2001; Hirai et al. 2002, 2004; Desgreniers et al. 2003; Sasaki et al. 2003). The transition pressures from cage structures to the FIIhS clearly correlate to the guest size; the larger the guest size, the higher the pressure at which the hydrate can be maintained. This suggests that larger guests are more favorable for holding the shrinking cages during compression (Hirai et al. 2004). In contrast, as for FIIhSs, there is no dependence of stability on the guest size. The decomposition pressures of FIIhSs are variable; only methane hydrate survives up to 40 GPa (Hirai et al. 2003, 2004), while other gas hydrates decompose below 6.5 GPa. Although methane has the largest size among the reported guest species forming FIIhSs, its retention under extremely high pressure cannot be explained only by its size. The reason for the stability of the methane hydrate FIIhS has not yet been clarified.

A theoretical study using the first principle calculation reported the retention of the FIIhS of methane hydrate up to 100 GPa (Iitaka and Ebisuzaki 2003). Here, interesting points

* E-mail: hhirai@sakura.cc.tsukuba.ac.jp

0003-004X/06/0506–826$05.00/DOI: 10.2138/am.2006.1991

arise whether the FIIhS of methane hydrate survives above 40 GPa or a certain post filled-ice-Ih structure (post-FIIhS) exists, and why only the FIIhS of methane hydrate is sustained under such high pressure. In this study, high-pressure experiments of methane hydrates were performed in the pressure range from 0.2 GPa to 86 GPa using X-ray diffractometry (XRD) and Raman spectroscopy. The XRD revealed a structural change at about 40 GPa, and Raman spectroscopy showed increased attractive interaction between methane and water molecules of the host framework above 15 GPa, which may explain the additional retention of the FIIhS.

Experimental procedure

A lever-and-spring type diamond anvil cell (DAC) was used in the high-pressure experiments. The ruby fluorescence method was used for the pressure measurements. The accuracy of the present measurement system is 0.1 GPa, taking the resolution of the spectrometer and the analytical procedure into account. The XRD study was performed using synchrotron radiation on BL-18C and BL-13A at the Photon Factory, High Energy Accelerator Research Organization (KEK). A monochromatized beam with a wavelength of 0.6198 Å was used. The starting material was methane hydrate powder, which was prepared using a conventional ice-gas interaction method under 15 MPa and –3 °C. This powder consisted of almost pure methane hydrate with full occupancy and did not contain excess water content, according to a combustion analysis. The relative intensities of the XRD peaks of this powder showed good agreement with those of the full-occupancy model of the sI. The sample powder was placed into a gasket hole in a vessel cooled by liquid nitrogen to prevent the decomposition of the sample. It was sealed by loading the anvils to approximately 0.2 GPa at a low temperature, and then the DAC was warmed to room temperature. XRD and Raman studies and optical observations were conducted at room temperature in a pressure range from 0.2 to 86 GPa.

Results

Under an optical microscope, no change was detected by visual inspection through the pressure range after the transition from the sH to the FIIhS at 2.0 GPa. In the XRD patterns, typical diffraction peaks of 011, 110, 002, 121, 112, 013, 132, and 123 of the FIIhS were observed under the pressures below 40 GPa, although the XRD patterns became somewhat broad as observed in the previous study (Hirai et al. 2003) (Fig. 1a). The XRD patterns were confirmed not to change especially in the pressure range from 14 to 20 GPa even after an annealing treatment. On the other hand, the Raman spectra clearly changed in the pressure range as described below. The diffraction peaks observed below 40 GPa were indexed as the FIIhS within very small deviations (<0.1%). The peaks of ice VII observed in Figure 1 were attributed to water released from the starting sI as a result of the structural changes. The molecular ratios of H_2O:CH_4 are 5.75:1 for the sI and 2:1 for the FIIhS, respectively. Thus, the amount of water corresponding to the difference is released above 2 GPa, which transforms to ice VII. At 40 GPa, four new peaks began to appear: one at a slightly higher angle than 002, one at a higher angle than 112, and two at lower angles than 123 (Fig. 1b). The relative intensities of these peaks increased above 40 GPa. Conversely, the remaining peaks (002, 121 and 123) weakened above 40 GPa and completely disappeared at 59.4 GPa (Fig. 1b). Above 60 GPa, only these four peaks had strong intensities. Figure 1c shows XRD patterns obtained by heat treatment up to 1000 K at 54.6 GPa (described below), showing the four peaks. The XRD patterns characterized by these four peaks were observed until 86 GPa. With decreasing pressure, the four peaks were observed until 40 or 35 GPa, and XRD patterns reverted to those observed below 40 GPa. This indicated that the transition at 40 GPa was reversible in spite of some hysteresis. The FIIhS was reproduced even after compression to 86 GPa. The same results were observed with good reproducibility in four experiments.

To check the possibility of decomposition of the FIIhS into solid methane and ice VII, additional high-pressure experiments were performed for solid methane in the pressure range from 1 to 86 GPa. The phase changes observed for solid methane were described elsewhere (Hirai et al., unpublished manuscript). The observed XRD patterns for the FIIhS were completely different from those of solid methane. The relative intensities of ice VII did not increase above 40 GPa. Thus, the observed XRD patterns were intrinsic to the high-pressure structure of methane hydrate. The heating experiments were carried out by using a CO_2-laser at 54.6 and 86 GPa. One objective of the heating was to examine the retention of the samples under high temperature and pressure. The temperature was estimated to be up to 1000 K. The high-pressure structure persisted up to 1000 K at 54.6 and 86 GPa. The second objective was to anneal the samples because the XRD patterns above 40 GPa were broad; however, the XRD patterns were not remarkably improved after heating.

Figure 2 shows Raman spectra of intramolecular vibration modes of methane i.e., the symmetric stretching mode ν_1 and the antisymmetric stretching mode ν_3. Figure 3 shows variations in the Raman shift of these modes with increasing pressure. The Raman shifts of the vibration modes increased, in general, with increasing pressure, but significant changes were observed at approximately 15 and 40 GPa. At 14 to 17 GPa, both ν_1 and ν_3 peaks began to split; new peaks appeared at lower frequencies, indicating formation of softer vibration modes (Fig. 2b). The new ν_1 peak became gradually dominant. The original ν_1 peak weakened but remained until about 55 GPa (Fig. 3). As pressure was decreased, this peak returned at about 18 GPa. The new ν_3 peak became strong above 20 GPa (Fig. 2). The original ν_3 peak was observed to 86 GPa under increasing pressure, in contrast to the original ν_1 peak. In addition to the distinct peak-splits, discontinuous changes in the slopes of the Raman shift were observed at about 40 GPa (Fig. 3). The peak splits and discontinuous changes in the slopes were observed both in increasing and decreasing pressure, indicating that these changes occurred reversibly.

Discussion

The XRD and Raman studies revealed that several changes took place in the methane hydrate samples at approximately 15 and 40 GPa. The change at about 15 GPa was observed only in Raman spectra, while the XRD patterns remained unchanged at around 15 GPa. Thus, this change is interpreted as the change in the vibration modes of methane molecule within the same fundamental structure of FIIhS. The change at 40 GPa was observed both in the XRD patterns and Raman spectra. This implies that the fundamental structure changed from the FIIhS to a post-filled-ice-Ih structure (post-FIIhS) at 40 GPa, and that the change of vibration modes was induced by the structural change. The theoretical study using the first principle calculation reported that the FIIhS can be stabilized to 100 GPa (Iitaka

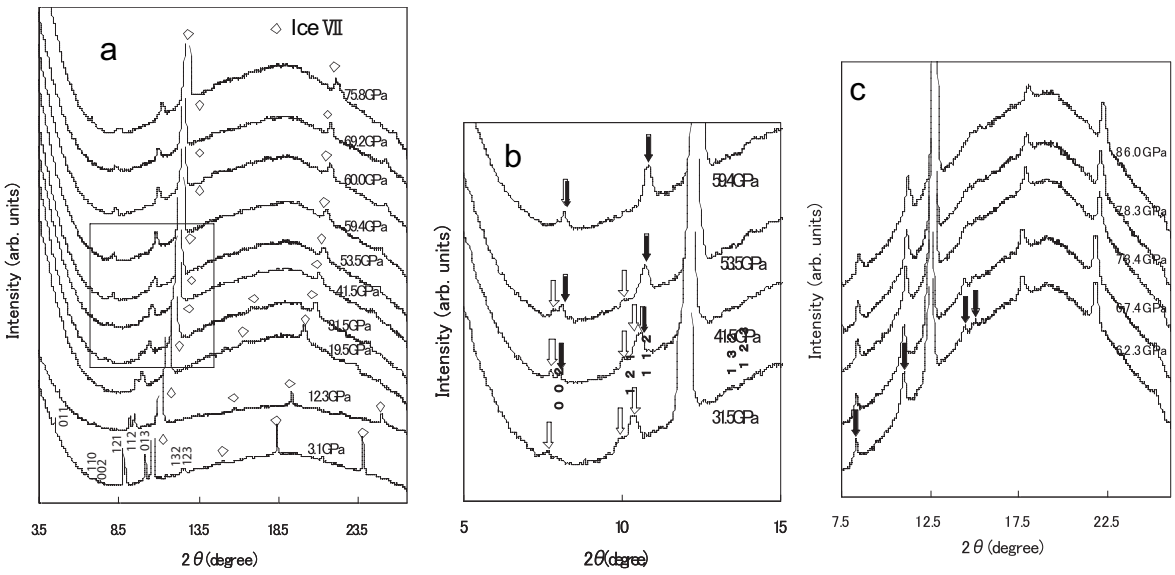

FIGURE 1. (**a**) Representative X-ray diffraction patterns with increasing pressure. (**b**) Enlargement of a square drawn in **a**, showing that new peaks (marked by solid arrows) begin to appear as original peaks (marked by open arrows) disappear. (**c**) X-ray diffraction patterns above 60 GPa obtained by an annealing treatment, showing the presence of new peaks.

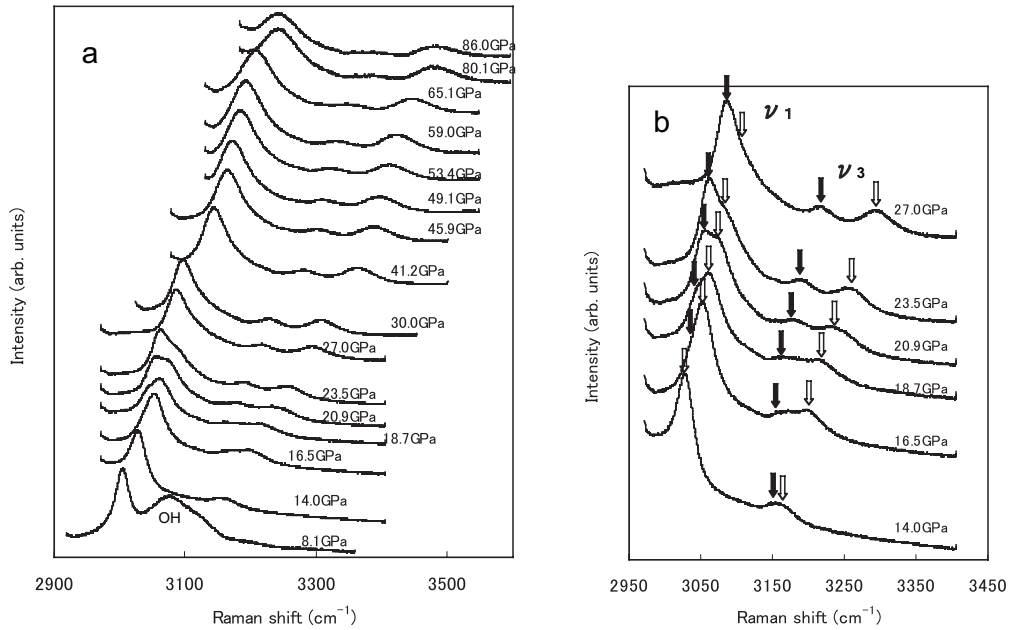

FIGURE 2. (**a**) Raman spectra of intramolecular vibration modes, ν_1 and ν_3, for methane. (**b**) Enlargement of a part of **a**, showing peak split. New vibration modes (marked by solid arrows) appear at lower frequencies than original ones (marked by open arrows) for ν_1 and ν_3, respectively. Although the original ν_1 peaks are not very evident above 30 GPa, they can be recognized as asymmetric-shaped peak until about 55 GPa with increasing pressure.

and Ebisuzaki 2003). The lattice parameters calculated by the theoretical study below 40 GPa showed excellent agreement with those obtained experimentally by the present authors (Hirai et al. 2003; Iitaka and Ebisuzaki 2003). However, in the present study, a change in the XRD patterns was clearly observed above 40 GPa; thus, the retention of the FIIhS should be limited to pressures below 40 GPa.

As described above, the FIIhSs of other gas hydrates such as argon-, krypton-, and nitrogen-hydrate decompose at various pressures below 6.5 GPa. Only methane hydrate showed remarkable stability and persisted to 40 GPa. In the Raman spectra, the vibration modes, ν_1 and ν_3, stiffened in general with increasing pressure, but another new vibration modes softer than the original ones appeared at 14 to 17 GPa. The appearance of the softer vibration modes indicates that the methane molecules began to receive an additional intermolecular interaction between the

methane and the host water and also between methane molecules at the pressure region. Recently, a high-pressure study using IR measurements and theoretical calculations has just reported that symmetrization of hydrogen bonds occurs in the FIIhS at 12 to 19 GPa at room temperature (Klug et al. 2005). Symmetrization in ice VII has been well examined (e.g., Goncharov et al. 1999; Aoki et al. 1996). The additional interaction presently observed in the FIIhS occurs almost simultaneously with the symmetrization of the water molecules forming framework. Thus, the increased interaction might be induced by the symmetrization of the framework. The excellent stability of the FIIhS under very high pressures could be substantiated by the symmetrization of the framework and by the subsequent increased intermolecular interactions between the methane molecules and the framework, as well as between the methane molecules. A similar explanation was reported for the retention of hydrogen hydrate up to 280 K (Mao et al. 2002). In hydrogen hydrate, the vibration mode of hydrogen molecules was softer than those of other known phases in the H2-H2O system, which was explained as an indication of increased intermolecular interaction. This increased interaction contributes to additional stability even under 260 K and 200 MPa (Mao et al. 2002). The increased interaction presently observed in methane hydrate, as well as that reported in hydrogen hydrate (Mao et al. 2002), is thought to be an important factor in maintaining the stability of clathrates, FIIhSs, and post-FIIhSs under extreme conditions.

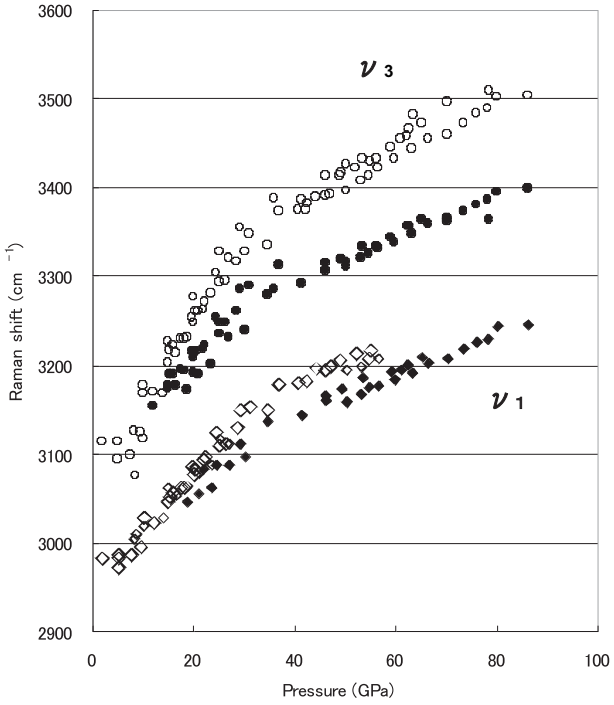

FIGURE 3. Variation of Raman shift of ν_1 and ν_3 with pressure. Besides the split at about 15 GPa, discontinuous changes in slope are observed at about 40 GPa.

As for the post-FIIhS above 40 GPa, we attempted to examine the structure using the four new diffraction lines, although the number of diffraction lines was limited. These lines were somewhat broad but clearly observed along Debye-rings. At first, we tentatively indexed the new peaks as the FIIhS because the new peaks appeared close to the original peaks. In that indexing, however, the deviations between the calculated d-values and the observed ones were considerable large, up to 4%. In addition, the volume calculated became larger than that of the FIIhS at 40 GPa. Thus, that indexing was quite unreasonable. Two possible indexing schemes were suggested. Initially, indexing was based on orthorhombic symmetry with the lattice parameters a = 4.069 Å, b = 6.890 Å, c = 5.976 Å at 50.6 GPa. In this case, the deviations between the observed d-values and calculated ones were very small through the pressure range (Table 1). These lattice parameters were almost the same as those calculated for the

TABLE 1. Two possible indexing of diffraction lines for the post-FIIhS

	$h\,k\,l$	d_{obs} (Å)	d_{calc} (Å)	d_o/d_c^{-1}	$h\,k\,l$	d_{obs} (Å)	d_{calc} (Å)	d_o/d_c^{-1}
50.6GPa								
	0 2 1	2.9847	2.9847	0.0000	1 0 1	2.9847	2.9896	–0.0016
	0 2 2	2.2572	2.2572	0.0000	1 1 2	2.2572	2.2540	0.0014
	0 4 0	1.7226	1.7226	0.0000	1 3 2	1.7226	1.7225	0.0001
	1 3 2	1.6621	1.6621	0.0000	1 2 3	1.6621	1.6626	–0.0003
62.5GPa								
	0 2 1	2.9451	2.9441	0.0003	1 0 1	2.9451	2.9461	–0.0004
	0 2 2	2.2225	2.2226	0.0000	1 1 2	2.2225	2.2218	0.0003
	0 4 0	1.7015	1.7015	0.0000	1 3 2	1.7015	1.7015	0.0000
	1 3 2	1.6395	1.6395	0.0000	1 2 3	1.6395	1.6396	–0.0001
69.7GPa								
	0 2 1	2.9199	2.9211	–0.0004	1 0 1	2.9199	2.9354	–0.0053
	0 2 2	2.2065	2.2064	0.0001	1 1 2	2.2065	2.1996	0.0045
	0 4 0	1.6876	1.6876	0.0000	1 3 2	1.6876	1.6873	0.0002
	1 3 2	1.6138	1.6138	0.0000	1 2 3	1.6138	1.6154	–0.0010
76.8GPa								
	0 2 1	2.8943	2.8982	–0.0014	1 0 1	2.8943	2.8958	–0.0005
	0 2 2	2.1840	2.1836	0.0002	1 1 2	2.1840	2.1830	0.0004
	0 4 0	1.6778	1.6777	0.0001	1 3 2	1.6778	1.6778	0.0000
	1 3 2	1.6114	1.6114	0.0000	1 2 3	1.6114	1.6116	–0.0001
80.3GPa								
	0 2 1	2.8701	2.8618	0.0029	1 0 1	2.8701	2.8784	–0.0029
	0 2 2	2.1674	2.1683	–0.0004	1 1 2	2.1674	2.1621	0.0025
	0 4 0	1.6490	1.6493	–0.0002	1 3 2	1.6490	1.6488	0.0001
	1 3 2	1.5904	1.5904	0.0000	1 2 3	1.5904	1.5912	–0.0005
Notes: a = 4.069(0) Å, b = 6.890(0) Å, c = 5.976(0) Å, V = 167.5(0) Å^3 at 50.6 GPa.					*Notes:* a = 3.344(13) Å, b = 7.554(23) Å, c = 6.671(19) Å, V = 168.5(9) Å^3 at 50.6 GPa.			

FIIhS in the theoretical study (Iitaka and Ebisuzaki 2003), but the extinction rules were completely different from that of FIIhS. The second indexing was also based on orthorhombic symmetry but with the lattice parameters $a = 3.344$ Å, $b = 7.554$ Å, $c = 6.671$ Å at 50.6 GPa, in which case the deviations of d-values were also small (Table 1). For this unit cell, the length of the *a*-axis was about two times that of the *c*-axis, indicating pseudo-tetragonal symmetry. The volumes above 50 GPa were a little larger by 1 to 3% than those calculated as the FIIhS above 50 GPa, but they were, of course, smaller than that of 40 GPa. In any case, the volume change was very small. Also, the relative intensity ratio of the post-FIIhS to the ice VII was almost the same as that of FIIhS to ice VII, i.e., the amount of ice VII did not increase or decrease at the transition. Thus, the molecular ratio of methane to water appears to be unchanged between the two structures. Considering the molecular ratio and the small volume change, the fundamental structure of the post-FIIhS might be not largely different from that of the FIIhS, although the true symmetry of the post-FIIhS cannot be determined at present because of the limited number of diffraction lines. This interpretation is consistent with the Raman spectra, which showed no evidence of peak splitting but only discontinuous changes in the slopes of the Raman shifts.

The presently observed stabilization of methane hydrate under extremely high pressure will contribute to a general understanding on gas hydrate stability. In addition, the finding of post-FIIhS of methane hydrate and of its persistence up to 86 GPa could help model the internal structure and the evolution of the giant planets such as Uranus and Neptune, and lead to new developments in ice-related material science. Detailed structural analyses of the post-FIIhS and its relationship to the vibration modes will be subjects of future study.

ACKOWLEDGMENTS

This work was supported in part by Grant-in-Aid for Science Research from the Ministry of Education, Culture, Sports, Science and Technology. We express our grateful acknowledgment to Takumi Kikegawa, High Energy Accelerator Research Organization, for his help on the synchrotron X-ray studies.

REFERENCES CITED

Aoki, K., Yamawaki, H., Sakashita, M., and Fujihisa, S. (1996) Infrared absorption study of the hydrogen-bond symmetrization in ice to 110 GPa. Physical Review B, 54, 15673–15677.

Chou, I.-M., Sharma, A., Burruss, R.C., Shu, J., Mao, H.K., and Hemley, R.J. (2000) Transformations in methane hydrates. Proceedings of the National Academy of Science, 97, 13484–13487.

Circone, S., Stern, L.A., and Kirby, S.H. (2004) The effect of elevated methane pressure on methane hydrate dissociation. American Mineralogist, 89, 1192–1201.

Desgreniers, S., Flacau, R., Klug, D.D., and Tse, J.S. (2003) Dense noble gas hydrates: phase stability and crystalline structures. Abstract of the International Conference of CeSMEC, Miami, March 24–28. Florida International University Press, Miami, Florida.

Goncharov, A.F., Struzhkin, V.V., Mao, H.K., and Hemley, R.J. (1999) Raman spectroscopy of dense H_2O and the transition to symmetric hydrogen bonds. Physical Review Letters, 83, 1998–2001.

Hirai, H., Uchihara, Y., Fujihisa, H., Sakashita, M., Katoh, E., Aoki, K., Nagashima, K., Yamamoto, Y., and Yagi, T. (2001) High-pressure structures of methane hydrate observed up to 8 GPa at room temperature. Journal of Chemical Physics, 115, 7066–7070.

——— (2002) Structural changes of argon hydrate under high pressure. Journal of Physical Chemistry B, 106, 11089–11092.

Hirai, H., Tanaka, T., Kawamura, T., Yamamoto, Y., and Yagi, T. (2003) Retention of filled ice structure of methane hydrate up to 42 GPa. Physical Review B, 68, 172102–1 –172102-4.

Hirai, H., Tanaka, T., Kawamura, T., Yamamoto, Y., and Yagi, T. (2004) Structural changes in gas hydrates and existence of a filled ice structure of methane hydrate above 40 GPa. Journal of Physics and Chemistry of Solids, 65, 1555–1559.

Hoffman, P.F., Kaufman, A.J., Halverson, G.P., and Schrag, D.P. (1998) A Neoproterozoic snowball Earth. Science, 281, 1342–1346.

Hubbard, W.B. (1997) Neptune's deep chemistry. Science, 275, 1279–1280.

Iitaka, T. and Ebisuzaki, T. (2003) Methane hydrate under high pressure. Physical Review B, 68, 172105-1–172105-4.

Jeffrey, G.A. (1984) Hydrate inclusion compounds. In J.L. Atwood, J.E.D. Davis, and D.D. MacNicol, Eds., Inclusion Compounds, p. 135–190. Academic Press, London.

Jiang, G., Kennedy, M.J., and Christie-Blick, N. (2003) Stable isotopic evidence for methane seeps in Neoproterozoic postglacial cap carbonates. Nature, 426, 822–826.

Klug, D.D., Tse, J.S., Liu, Z., Mao, H.-K., Hemley, R.J. (2005) Infrared study of symmetric hydrogen bond formation in the methane clathrate. Oral presentation at Joint 20th AIRAPT-43rd EHPRG Conference on Science and Technology of High Pressure, Karlsruhe, Germany, June 27th–July 1st, 2005.

Kurnosov, A.V., Manakov, A.Y., Komarov, V.Y., Voronin, V.I., Teplykh, A.E., and Dyadin, Y.A. (2001) A new Gas hydrate structure. Doklady Physical Chemistry, 381, 303–305.

Kvenvolden, K.A. (1988) Methane hydrate—A major reservoir of carbon in the shallow geosphere? Chemical Geology, 71, 41–51.

Loveday, J.S., Nelmes, R.J., Guthrle, M., Belmonte, S.A., Allan, D.R., Klug, D.D., Tse, J.S., and Handa, Y.P. (2001a) Stable methane hydrate above 2 GPa and the source of Titan's atmospheric methane. Nature, 410, 661–663.

Loveday, J.S., Nelmes, R.J., Guthrie, M., Klug, D.D., and Tse, J.S. (2001b) Transition from cage clathrate to filled ice: the structure of methane hydrate III. Physical Review Letters, 87, 215501-1–215501-4.

Mao, W.L., Mao, H.K., Goncharov, A.F., Struzhkin, V.V., Guo, Q., and Hemley, R.J. (2002) Hydrogen clusters in clathrate hydrate. Science, 297, 2247–2249.

Olszewski, T.D. and Erwin, D. (2004) Dynamic response of Permian brachiopod communities to long-term environmental change. Nature, 428, 738–741.

Ripmeester, J.A., Tse, J.S., Ratcliffe, C.I., and Powell, B.M. (1987) A new clathrate hydrate structure. Nature, 325, 135–136.

Shimizu, H., Kumazaki, T., Kume, T., and Sasaki, S. (2002) In-situ observations of high-pressure phases transformations in a synthetic methane hydrate. Journal of Physical Chemistry B, 106, 30–33.

Sloan, E.D. (1998) Clathrate Hydrates of Natural Gases (2nd edition). Marcel Dekker Inc., New York.

——— (2004) Introductory overview: Hydrate knowledge development. American Mineralogist, 89, 1155–1161.

Stern, L.A., Kirby, S.H., and Durham, W.B. (1996) Peculiarities of methane hydrate formation and solid-sate deformation, including possible superheating of water ice. Science, 273, 1843–1848.

Waite, W.F., Winters, W.J., and Mason, D.H., Methane hydrate formation in partially water-saturated Ottawa sand. American Mineralogist, 89, 1202–1207.

MANUSCRIPT RECEIVED MAY 30, 2005
MANUSCRIPT ACCEPTED DECEMBER 21, 2005
MANUSCRIPT HANDLED BY GEORGE LAGER